EXPERIMENTAL AND NUMERICAL INVESTIGATIONS OF THE FAILURE BEHAVIOUR OF COMPONENTS BY APPLICATION OF FRACTURE AND DAMAGE MECHANICS

W. Baer [1] and D. Klingbeil [1]

[1] Division V.3 Service Loading Fatigue and Structural Integrity,
Federal Institute of Materials Research and Testing (BAM),
Unter den Eichen 87, 12205 Berlin, Germany

ABSTRACT

Modern safety analysis of components focuses on providing safety margins on the basis of the quantification of the failure process. Within this scope the investigations that are presented deal with the development and verification of a method for the realistic prediction of displacements in components due to service loads, amounts of crack growth and especially crack opening displacements. A series of four-point bending tests on pipes made of 15NiCuMoNb5 steel with external circumferential surface flaws was carried out until leakage and final cleavage failure. The large set of purposefully determined data gave detailed information about the behaviour of the component in service and was needed for the development and verification of finite element models. Several engineering approaches were used to provide and to compare analytical predictions of the pipe failure. The tests performed on pipes with a 90°-external circumferential flaw were analyzed by the finite element method and by a damage model taking ductile crack growth into account. The simulation of the ductile crack growth was performed up to the experimentally observed instability of the pipe. The numerically determined crack opening area was identical with the experimental result. The numerically determined stress triaxiality as well as the crack opening stress achieved maximum values at the same position in the pipe and at the same time where experimental cleavage failure was initiated. It was shown by the finite element analysis of ductile crack growth that even complex failure of components can be modelled in the right way. It is pointed out that the problem could only be solved by damage models as conventional fracture mechanical concepts are not suited to be applied for large ductile crack growth.

INTRODUCTION

One of the basic problems within the safety analysis of components is the lack of valid crack resistance curves for large amounts of crack growth due to the validity margins in the relevant standard procedures and the uncertainty of how to extrapolate the curves correctly. The assessment tools for the elastic plastic material and component behaviour have been significantly improved by the development of micromechanical material models which cover damage evolution during the ductile fracture process. Advantages of these models are geometry independent material parameters and their validity even with large amounts of ductile crack growth.

EXPERIMENTAL AND NUMERICAL INVESTIGATIONS

Material

The material under investigation was the 15NiCuMoNb5 ferritic-bainitic high-temperature structural steel (WB36) in the form of seamless pipes with nominal dimensions of length * outer diameter * thickness = 2000 * 273 * 16 mm³. The chemical composition corresponded to the increased requirements for 15NiCuMoNb5S in terms of sulphur and phosphorus according to German KTA 3211.1 specification [1]. Table 1 shows mechanical and fracture mechanical properties of the investigated material at ambient temperature together with Charpy impact energy values. Crack initiation toughness values J_i were determined on the basis of the critical stretch zone width from crack resistance curves of fatigue precracked and 20%-sidegrooved C(T)6.25 specimens in L-S orientation with initial crack length ratio of 0.5 (L – axial direction in the pipe, T – tangential direction, S – wall thickness direction) according to the ESIS P2-92 guideline [2].

TABLE 1
MECHANICAL AND FRACTURE MECHANICAL PROPERTIES OF THE INVESTIGATED 15NiCuMoNb5 STEEL AT AMBIENT TEMPERATURE

	$R_{p0,2}$ [MPa]	R_m [MPa]	A [%] (L-direction)	K_V [J]	K_{VH} [J]	J_i [N/mm]
Nominal value for 15NiCuMoNb5S according to [1]	≥ 440	610-760	≥ 19	≥ 95 [1]) ≥ 66 [2]) (20 °C, T-L)	100 [2])	-
Actual value	515	672	27	-	-	-
Actual value, T-L-position	-	-	-	105 [1]) (20 °C) 98 [2]) (20 °C)	159	-
Actual value, L-S-position	-	-	-	133 ± 15 (22 °C, 8 Proben)	176	126

[1]) mean value of 3 specimens, [2]) lowest single value

Pipe Bending Tests

The pipe test program [3] covered one test on a pipe with no flaw (pipe no. 4), two tests on pipes with 90°-external circumferential surface flaws (pipe no. 2 and 5) and one test on a pipe with 60°-external circumferential surface flaw (pipe no. 1) each of which with initial flaw depth ratios of 0.5 (Figure 1). The numerical investigations applied to the experimental data of the test on pipe 2 with 90°-flaw. Figure 1 gives a schematic outline of the test stand for pipe bending tests that was built up in a 20 MN servohydraulic testing machine. The pipes had been extensively instrumented with inductive linear position transducers and clip gages in order to provide a large set of purposefully determined data of deflection, ovalization and crack opening displacement (COD) that was needed for the development and verification of finite element models.
A number of non-destructive testing methods were applied focussing on the investigation of the crack growth and leakage behaviour of the pipes. Ultrasonic testing, acoustic emission testing, direct current potential drop technique and an optical analysis delivered detailed data on the experimental pipe failure. Several engineering approaches were used to compare the predictions of the failure of two pipes, with 60°- and 90°-flaw, in terms of load in comparison to the experimental maximum failure loads: Plastic Limit Load Concept, Concept of Local Flow Stress, R6 Procedure and Engineering Treatment Model. The relevant equations as well as the assumptions and boundary conditions used are described in detail in [3].

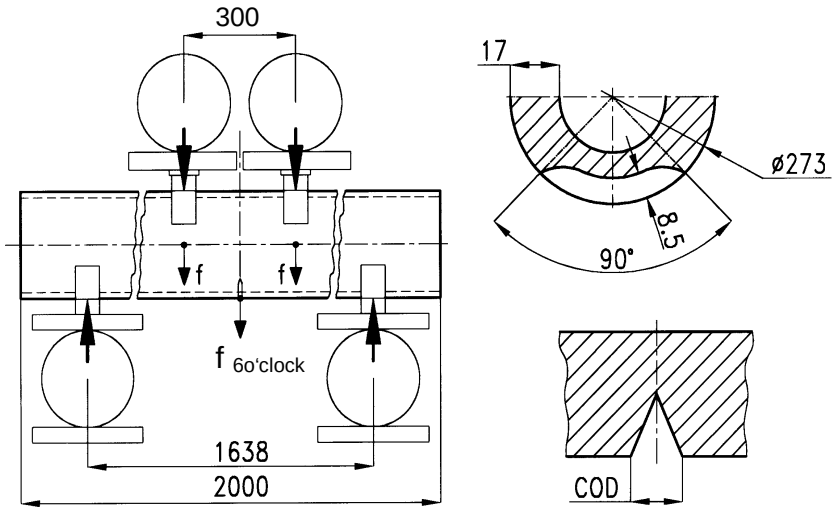

Figure 1: Schematic outline of the test stand for pipe bending tests and position of selected gauging points (f – deflection, COD – crack opening displacement)

Finite Element Analysis

The numerical analysis of the failure behaviour of pipe no. 2 with 90°-external circumferential surface flaw was performed by three-dimensional finite element analysis (FEA) using the damage model of GURSON modified by NEEDLEMAN and TVERGAARD [4] for the simulation of ductile crack growth. Table 2 summarizes the geometry independent material parameters of the applied damage model for the investigated steel 15NiCuMoNb5 at ambient temperature that were determined by fitting them for experimental results of tensile tests on notched bars with different notch radii as well as for one experiment on a C(T)6.25 specimen.

TABLE 2
MATERIAL PARAMETERS DETERMINED FOR DUCTILE DAMAGE AND FAILURE OF 15NiCuMoNb5 STEEL AT AMBIENT TEMPERATURE

f_a	f_n	ε_n	s_n	f_c	f_f
0,0001	0,008	0,25	0,1	0,022	0,19

The geometry of the pipe and the bearings had to be modelled very exactly to achieve the experimentally measured forces and displacements and had therefore been optimized by experimental data of the test with the unflawed pipe no. 4. Due to the limited available computer capacity the pipe with 90°-flaw was meshed by three-dimensional elements with linear shape functions and approximate edge length of 0.25 mm in radial (y) as well as axial (x) direction and 2.2 mm in tangential direction (z), see Figure 2.

RESULTS AND DISCUSSION

The experimental failure behaviour of the pipes with 60°- and 90°-flaws in the displacement controlled tests was characterized by ductile crack growth until full penetration of wall thickness (leakage), growth of the leak and final instability by brittle fracture. The analysis of the fracture surfaces proved that stable crack growth in circumferential direction beyond the angle of the machined initial flaw did not occur, see Figure 3. The cleavage fracture initiation region was always located in the area in front of the initial flaw angle.

All of the applied engineering approaches for the assessment of the failure behaviour of the pipes no. 1 with 60°-flaw and no. 2 with 90°-flaw provided conservative predictions of the pipe instability, i.e. smaller loads than experimentally detected, see Table 3. Table 3 shows that the Engineering Treatment Model and the

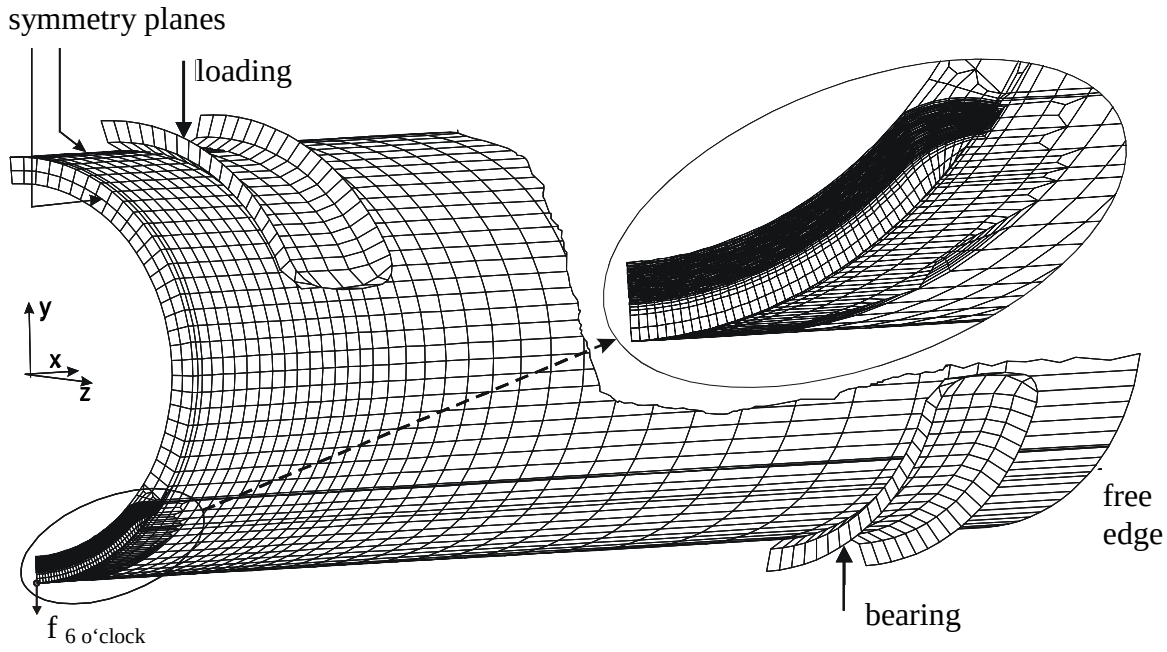

Figure 2: Finite element mesh of pipe no. 2 with 90°-external circumferential surface flaw, rigid bearings and contact

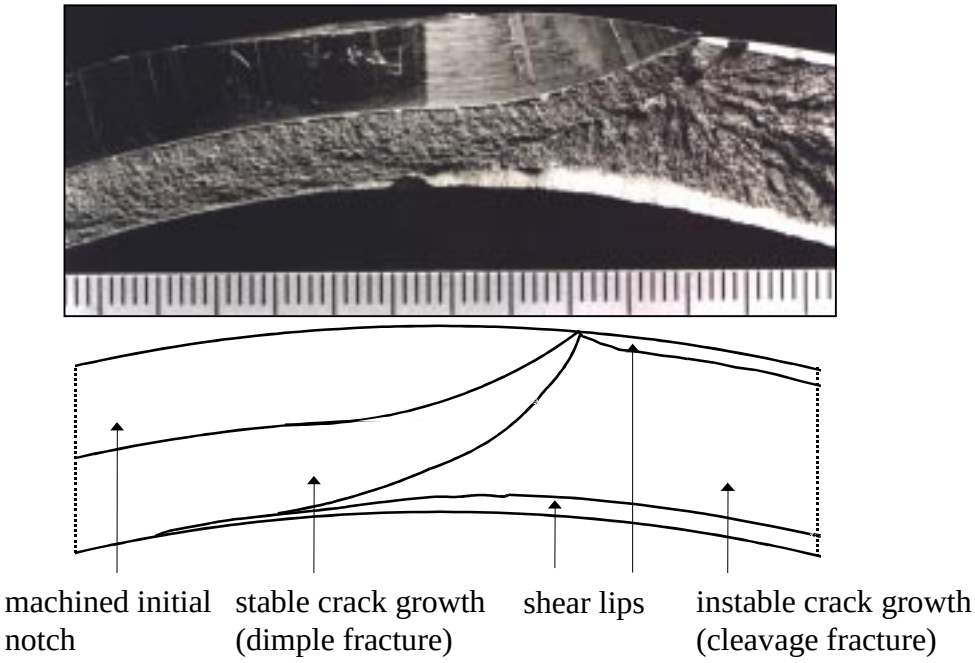

Figure 3: Sector of the fracture surface of pipe no. 2 with 90°-flaw, 1 scale division equals 1 mm

R6 Procedure with category 3, option 2 assessment curve, provided comparable results with the lowest level of conservatism. Despite the relative small input the Plastic Limit Load Concept gave a rather exact prediction of instability which only insignificantly drops below the level of exactness of the R6 category 3 analysis. The consideration of a correction of the yield load due to ovalization according to [5] leads to an increase in the safety margin or in the conservativeness of the failure prediction.

The finite element analysis of pipe no. 2 was performed until a maximum displacement of about 18 mm at which the experimental failure by cleavage fracture was observed. Within these analysis limits the simulated ductile crack growth led to a total leakage angle of about 70° in circumferential direction. It was proven by this that the experimental crack initiation and crack growth behaviour as well as the leakage behaviour of the

flawed pipe (Figure 3) was very well reproduced by the finite element analysis both in terms of the amounts of crack growth and the crack front shape.

TABLE 3
PREDICTION OF FAILURE BY ENGINEERING CONCEPTS AND EXPERIMENTAL FAILURE LOADS OF THE PIPES NO. 1 AND 5 WITH 60°- AND 90°-FLAW RESPECTIVELY

	Experiment		Plastic Limit Load Concept	Local Flow Stress Concept	R6 Procedure				Engineering Treatment Model ETM	
					Option 1		Option 2			
	Crack initiation load [kN]	Maximum load [kN]	Failure load [kN]	Failure load [kN]	Cat. 1, Failure load [kN]	Cat. 3, Failure load [kN]	Cat. 1, Failure load [kN]	Cat. 3, Failure load [kN]	Crack initiation load [kN]	Instability load [kN]
					Without correction of ovalization					
60°	1390	1605	1498	1330	1290	1556	1454	1540		
90°	1220	1474	1390	1160	1218	1437	1365	1414		
					With correction of ovalization					
60°					1179	1367	1272	1345	1254	1346
90°					1138	1327	1245	1294	1214	1290

Figure 4 shows the leakage opening at the internal surface of the pipe in dependence on the circumferential angle at several levels of deflection at the 6 o'clock position.

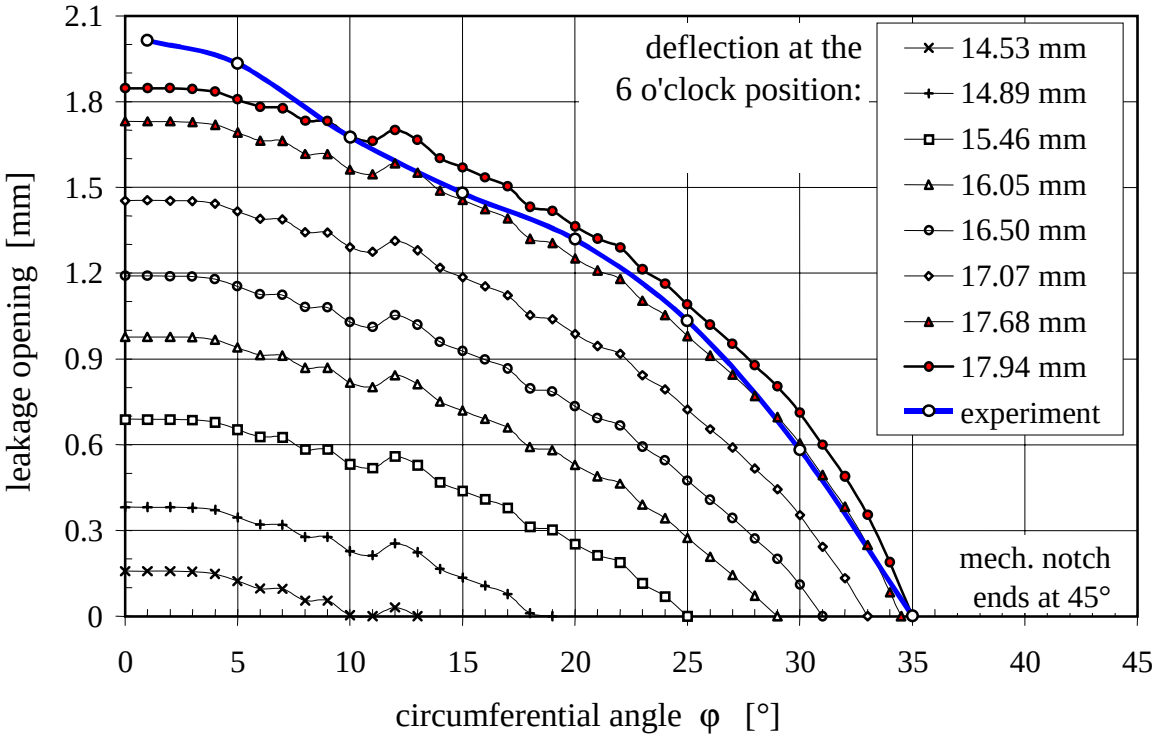

Figure 4: Pipe no. 2 with 90°-external circumferential surface flaw,
leakage opening profiles at different load levels in terms of deflection at the 6 o'clock position

Under the conditions of increasing deflection the maximum of the leakage opening at 0° (6 o'clock position) increases up to a value of about 1.8 mm and the leakage enlarges up to an angle of 35 ° in circumferential

direction. The numerically determined leakage opening profile in the moment of experimental failure at $f_{6o'clock}$ = 17.94 mm corresponds very well to the experimentally determined profile.
Two local maxima of the maximum stress triaxiality $\chi = \sigma_h/\sigma_v$ in the ligament, each of a value of about 2, are calculated at the beginning of the leakage, see Figure 5.

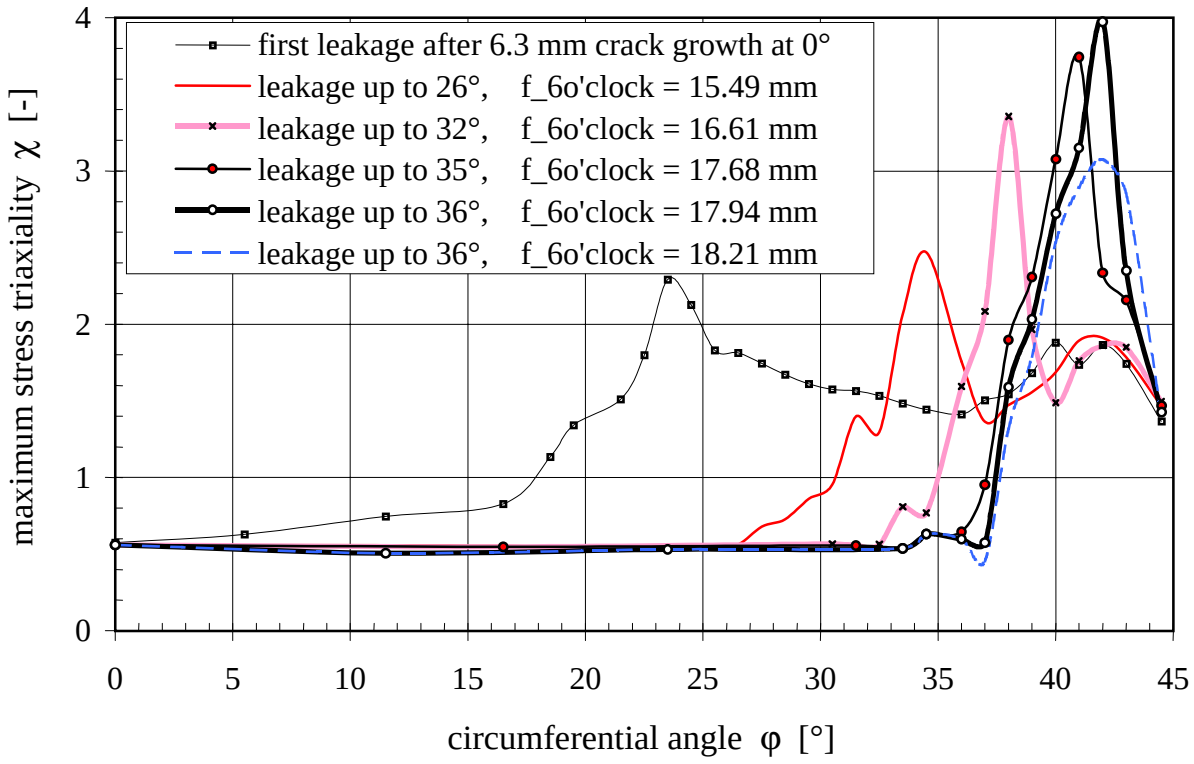

Figure 5: Pipe no. 2 with 90°-external circumferential surface flaw, maximum stress triaxiality in the ligament during leakage growth

The local maximum in front of the end of the crack at a circumferential angle of 40 to 45 ° remains during leakage growth. The second local maximum in front of the actual crack front is shifted in circumferential direction during crack growth, as the curves for leakage sizes of 26 ° and 32 ° show. At leakage sizes of 35 ° and 36 ° the local maxima merge to one global maximum with a value of stress triaxiality of about 4. Experimental crack instability by cleavage fracture was just observed at a leakage size of 36 ° ($f_{6o'clock}$ = 17,94 mm). This very high level of stress triaxiality was only determined at this position in the simulated structure and not until this stadium of the simulation of the test. All other values determined are significantly lower.
As can be seen from Figure 6, the position of the highest stress triaxiality coincides with the area on the fracture surface, where cleavage fracture was initiated (Figure 2). Therefore it is concluded that on the applied side the high stress triaxiality is responsible for the cleavage fracture that was initiated in the area in front of the crack at a circumferential angle of 40 to 45 °.

CONCLUSIONS

The comparison of experimentally and analytically determined failure loads shows that the applied engineering assessment concepts are practicable tools to give conservative and remarkably exact predictions of failure by instability. Especially the Engineering Treatment Model and the R6 Procedure, category 3 analysis, but also the Plastic Limit Load Concept provided good results while only comparatively small input

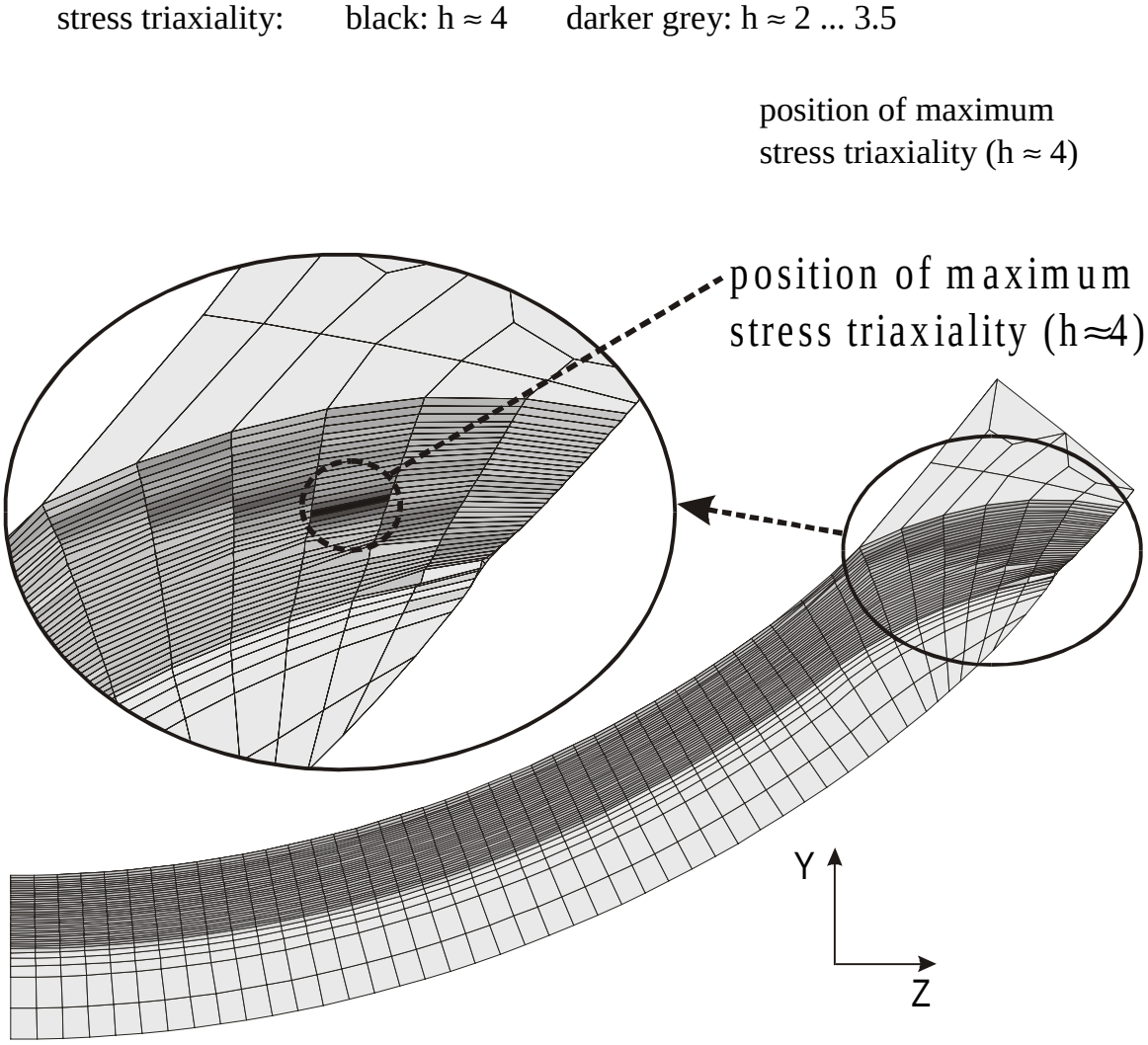

Figure 6: Pipe no. 2 with 90°-external circumferential surface flaw, maximum stress triaxiality in the ligament σ_h/σ_v at a deflection of $f_{6o'clock}$ = 17.94 mm, where experimental cleavage failure was observed

was needed. This underlines the necessity of improved engineering assessment concepts to enable the engineer to perform comparatively fast and straightforward analyses of flawed structures. However, more detailed analysis requires a higher amount of numerical work and is only possible by means of finite element methods.

In the present case it could be shown by the finite element analysis of ductile crack growth that even complex failure of components can be modelled in the right way. It is pointed out that the problem could only be solved by damage models as conventional fracture mechanics concepts are not suited to be applied for large ductile crack growth. The quality of the finite element analysis is shown because experimental and numerical results are nearly identical, which applies especially to the crack opening area. This is regarded as an important prerequisite for realistic assessment of effusion rates in damage cases and for the safety assessment of components in the field of power generating plants.

NOMENCLATURE

A	elongation at rupture
φ	circumferential angle (half of the total flaw angle)
COD	Crack Opening Displacement

$f_{6o'clock}$ deflection at the 6 o'clock position
J_i crack initiation toughness
K_V Charpy impact energy
K_{VH} upper shelf of Charpy impact energy
L axial direction (x-direction)
$R_{p0,2}$ 0.2% offset yield strength
R_m ultimate tensile strength
S wall thickness direction (y-direction)
σ_h hydrostatic stress
σ_v Mises effective stress
T tangential direction (z-direction)
f_n volume fraction of void nucleating particles
ε_n average plastic equivalent strain at which the nucleation of new voids reaches its maximum
s_n standard deviation of the distribution which controls the nucleation of new voids
f_a initial void volume fraction
f_c critical void volume fraction
f_f final void volume fraction

REFERENCES

1. Sicherheitstechnische Regel des KTA 3211.1 „Druck- und aktivitätsführende Komponenten von Systemen außerhalb des Primärkreises, Teil 1: Werkstoffe, Anhang A3: Ferritische Stähle der Werkstoffgruppe W I für nahtlose Rohre, nahtlose Rohrbogen und nahtlose Reduzierstücke“, Fassung April 1991
2. European Structural Integrity Society: ESIS Procedure for Determining the Fracture Behaviour of Materials. ESIS P2-92, Delft, Jan. 1992
3. Analyse und Weiterentwicklung bruchmechanischer Versagenskonzepte; Schwerpunkt: Anwendung fortgeschrittener zähbruchmechanischer Konzepte; Bruchübergang, Abschlußbericht zum Forschungsvorhaben BMBF 1500 970, Forschungsbericht 232, BAM Berlin, 1999
4. Needleman, A.; Tvergaard, V.: An Analysis of Ductile Rupture in Notched Bars. J. Mech. Phys. Solids 32 (1984), S. 461-490
5. Kanninen, M.F., Zahoor, A., Wilkowski, G., Abou-Sayed, I., Marshall, C., Broek, D., Sampath, S., Rhee, H. and J. Ahmad: Instability Predictions for Circumferentially Cracked Type 304 Stainless Steel Pipes under Dynamic Loading, EPRI Report NP-2347, 1982